Biogeosciences Discuss., 8, 6345–6382, 2011
www.biogeosciences-discuss.net/8/6345/2011/
doi:10.5194/bgd-8-6345-2011
© Author(s) 2011. CC Attribution 3.0 License.

Biogeosciences Discussions

This discussion paper is/has been under review for the journal Biogeosciences (BG).
Please refer to the corresponding final paper in BG if available.

Water table height and microtopography control biogeochemical cycling in an Arctic coastal tundra ecosystem

D. A. Lipson[1], D. Zona[1,2], T. K. Raab[3], F. Bozzolo[1], M. Mauritz[1], and W. C. Oechel[1]

[1]San Diego State University, San Diego, CA, USA
[2]University of Antwerp, Antwerp, Belgium
[3]Stanford University, Stanford, CA, USA

Received: 5 June 2011 – Accepted: 15 June 2011 – Published: 6 July 2011

Correspondence to: D. A. Lipson (dlipson@sciences.sdsu.edu)

Published by Copernicus Publications on behalf of the European Geosciences Union.

Abstract

Drained thaw lake basins (DTLB) are the dominant land form of the Arctic coastal plain in northern Alaska. The presence of continuous permafrost prevents drainage and so water tables generally remain close to the soil surface, creating saturated, suboxic soil conditions. However, ice wedge polygons produce microtopographic variation in these landscapes, with raised areas such as polygon rims creating more oxic microenvironments. The peat soils in this ecosystem store large amounts of organic carbon which is vulnerable to loss as arctic regions continue to rapidly warm, and so there is great motivation to understand the controls over microbial activity in these complex landscapes. Here we report the effects of experimental flooding, along with seasonal and spatial variation in soil chemistry and microbial activity in a DTLB. The flooding treatment generally mirrored the effects of natural landscape variation in water table height due to microtopography. Areas in the flooded areas had lower dissolved oxygen, lower oxidation-reduction potential (ORP) and higher pH, as did lower elevation areas of the landscape. Similarly, soil pore water concentrations of dissolved ferric iron (Fe III), organic carbon, and aromatic compounds were higher in flooded and low elevation areas. Dissolved carbon dioxide (CO_2) and methane (CH_4) concentrations were higher in low elevation areas. In anaerobic laboratory incubations, more CH_4 was produced by soils from low and flooded areas, whereas anaerobic CO_2 production only responded to flooding in high elevation areas. Seasonal changes in the oxidation state of solid phase Fe minerals showed that significant dissimilatory Fe reduction occurred, especially in topographically low areas. This suite of results can all be attributed to the effect of water table on oxygen availability: flooded conditions promote anoxia, stimulating anaerobic processes, methanogenesis and Fe(III) reduction. Flooding also increased soil temperature, which might account for the higher N mineralization rates and dissolved P concentrations observed in flooded areas, though the latter could also have resulted from solubilization of Fe-P minerals under more reducing conditions. Overall, the results indicate that the microbial community is well-adapted for anaerobic

BGD

8, 6345–6382, 2011

respiration, in particular, dissimilatory Fe(III) reduction, and could have implications for some high Arctic areas where warming and flooding are likely consequences of climate change.

1 Introduction

The height of the water table controls the balance of anaerobic and aerobic processes in wetlands and other periodically flooded systems (Blodau, 2002; Reddy and DeLaune, 2008; Kögel-Knabner et al., 2010). Surface water restricts the diffusion of oxygen (O_2), creating anoxic conditions that promote anaerobic processes such as methane (CH_4) production or anaerobic respiration using a variety of alternative electron acceptors, such as nitrate (NO_3^-), manganese (Mn(IV)), iron (Fe(III)), humic substances and sulfate (SO_4^{2-}). Surface water can also have other important physical effects on soils; for example in soils with thick surface organic layers, increased water content greatly increases thermal conductivity (Kujala et al., 2008; O'Donnell et al., 2009), and so flooding or ponding can lead to deeper heat penetration and active layer depth in soils with permafrost (Brown, 1967; Shiklomanov et al., 2010).

Northern permafrost soils contain vast reservoirs of carbon (C), and could be a major source for carbon dioxide (CO_2) and CH_4 in the next century as a result of climate warming (Schuur et al., 2008; Tarnocai et al., 2009). In the past century, high latitude sites have warmed faster than the rest of the planet (IPCC, 2007), and this warming trend has already caused significant increases in CH_4 production from Arctic ecosystems (Bloom et al., 2010). However, the specific responses of the Arctic C cycle to climate change, in particular the rates of ecosystem CH_4 and CO_2 production, will depend on complex interactions of factors such as microtopography and the availability of alternative electron acceptors with changes in temperature and hydrology.

The water table in many high Arctic ecosystems is affected by complex microtopographic patterns that arise from the formation of ice wedge polygons (Brown, 1967). Over many freeze-thaw cycles, ice wedges form in the soil, pushing up regions that

BGD
8, 6345–6382, 2011

become the rims of low-centered polygons, causing water to accumulate in the lower polygon centers. The ice wedges under the rims of these features can melt and subside, creating high centered polygons (Billings and Peterson, 1980). The presence of this complex spatial pattern complicates predictions of the ecosystem response to climate change. Previous studies have shown that the net effect of water table manipulations on the C cycle depend on the plant community and location on the landscape (Updegraff et al., 2001; Strack et al., 2006; Strack and Waddington, 2007). Furthermore, climate change will have complex effects on the hydrology of northern soils. As northern latitudes have warmed, areas of discontinuous permafrost have degraded, leading to draining of lakes; however in areas of continuous permafrost lake coverage has increased due to ground slumping as a result of themokarst activity (Smith et al., 2005). Predicting ecosystem responses to climate change in the Arctic requires an understanding of how water table and microtopography control biogeochemical cycling and microbial processes such as respiration and methanogenesis.

Drained thaw lake basins (DTLB) make up a significant portion of the landscape of the Arctic coastal plain (Billings and Peterson, 1980; Hinkel et al., 2003; Bockheim et al., 2004). These features originate as lakes that drain due to various erosional processes and become vegetated. As these DTLB develop over the course of hundreds to several thousand years, ice wedge polygons create complex topography within these basins. One such DTLB near Barrow, Alaska was the location of a large scale water table manipulation ("Biocomplexity") experiment (Zona et al., 2009; Olivas et al., 2010). Previous work at the Biocomplexity site showed that much of the basin is prone to anoxia, and that dissimilatory Fe(III) reduction is a particularly important anaerobic process that contributes significantly to the ecosystem C budget (Lipson et al., 2010). Despite the general tendency for this process to competitively inhibit methanogenesis (Roden and Wetzel, 1996; Blodau, 2002; Bond and Lovley, 2002; Küsel et al., 2008; Jerman et al., 2009), CH_4 production has also been detected in this ecosystem (Rhew et al., 2007; Zona et al., 2009; von Fischer et al., 2010). What factors allow the coexistence of these two potentially competing processes remains an open question (van

BGD
8, 6345–6382, 2011

Hulzen et al., 1999; Yavitt and Seidman-Zager, 2006; Keller and Bridgham, 2007; Knorr and Blodau, 2009).

The goal of this study was to understand the effects of natural and experimental variation in water table height on soil chemistry, microbial respiratory processes and nutrient cycling in polygonized tundra of the Arctic coastal plain in Northern Alaska. The motivation was to understand potential responses to climate change but also the controls of microtopography and water table height on the current functioning of this ecosystem.

2 Methods

2.1 Site description and flooding treatment

This research was carried out in a DTLB in the Barrow Environmental Observatory near Barrow, Alaska (71.32° N, 156.62° W). The DTLB is classified as medium aged, having drained from 50–300 years in the past (Hinkel et al., 2003). Low-centered polygons have formed over much of the basin, particularly in the central and north sections. Vegetation is dominated by mosses (*Sphagnum* spp.), sedges (*Carex aquatilis*, *Eriophorum* spp.), and grasses (*Dupontia fisheri, Arctophila fulva*), with mosses dominating topographically high areas such as polygon rims and *Carex* dominating low areas such as polygon centers (Zona et al., 2009; Olivas et al., 2010). The soils within the basin are classified as aquahaplels, orthels and histoturbels, with an organic horizon (~12–15 cm thick) overlaying a silty mineral layer. The active layer is typically about 30 cm deep (Shiklomanov et al., 2010). The water table manipulation experiment at this site has been described in detail previously (Zona et al., 2009; Lipson et al., 2010; Olivas et al., 2010). Briefly, the roughly elliptical basin (about 1.5 km long) was divided into three sections by plastic dikes buried in the permafrost. The north section was designated as the flooded treatment, the central originally as the draining treatment and the south as the control. Water was pumped from the central section into the north

BGD
8, 6345–6382, 2011

section. However this produced only modest alterations of the water table and so additional water was pumped into the north section from nearby Cakeeater Lake. This treatment was performed during the summers of 2008 and 2009. The draining treatment was very subtle in its effect on water table relative to the flooding treatment, and the control (south) and drained (central) areas were indistinguishable in the response variables measured in this study. Therefore the two non-flooded areas were pooled for most purposes in this study. Raised boardwalks were installed across each of the three sections, creating 300 m long transects. Elevation was recorded with a differential GPS (Trimble R7 and R8) every 2 m along each transect, and interpolated linearly as needed. All measurements presented here occurred along these three transects.

2.2 Soil electrochemistry

pH and oxidation-reduction potential (ORP) were measured at 10 cm depth using a portable meter and electrodes (Thermo-Orion). Electrodes were inserted into the soil after a small incision was made with a serrated knife. These measurements were made repeatedly at a set of permanent plots chosen to represent high and low areas of the landscape within each transect (three high and three low areas per transect, 18 total). These were the same locations used for soil pore water sampling described below. Additionally, more spatially intensive measurements were made on a subset of sampling days. ORP measurements are reported as raw values relative to the internal Ag/AgCl reference electrode. Dissolved O_2 was measured using a microelectrode and portable picoammeter (Unisense). The O_2 electrode was used to find the approximate location of the transition zone between oxic and anoxic horizons ("oxycline"). Because the electrode is only 5 cm long, if the oxycline lay deeper than 5 cm, it was recorded whether the dissolved O_2 concentration at 5 cm depth was suboxic (<50 % saturation) or oxic (>50 % saturation), and assigned non-parametric values 6 or 7, respectively.

BGD
8, 6345–6382, 2011

2.3 Soil water chemistry

Soil water was collected from 10 cm long, porous soil moisture samplers (Rhizon, Ben Meadows) inserted into the soil at an angle, to capture 0–5 cm soil pore water, or vertically, to capture water at 5–15 cm depths. The deeper depths were only accessible for a limited number of dates later in the season. The soil moisture samplers were installed in six locations on each transect, split between high and low areas as described above. Water samples were collected through hypodermic needles into evacuated tubes (BD Vacutainers). On most dates, two sets of water samples were collected; one was acidified with a drop of 1M HCl to preserve the oxidation state of dissolved Fe species. The other set, reserved for dissolved gas analysis, was not acidified and was sealed in Bitran bags to reduce gas exchange with the atmosphere. All water samples were kept refrigerated until analysis.

Acidified water samples were analyzed for dissolved Fe^{2+} and Fe^{3+} using 1,10-phenanthroline, as described previously (Analytical Methods Committee, 1978; Lipson et al., 2010). As an index of dissolved aromatic compounds, absorbance at 260 nm (A260) was measured on a standardized volume (200 µl) in UV-transparent microtiter plates using a microplate reader (SpectraMax 190, Molecular Devices). Dissolved organic C was measured using an assay based on Mn(III) as described earlier (Bartlett and Ross, 1988; Lipson et al., 2010).

Ammonium (NH_4^+) was analyzed using a phenolate-hypochlorite method and free amino-N, using a ninhydrin method (Lipson et al., 1999). Ninhydrin also reacts with NH_4^+ so these values were subtracted from ninhydrin-active N to yield amino-N. Phosphate (PO_4) was analyzed with a paramolybdate-ascorbate method (Kuo, 1996). All these assays were scaled down for use in a microplate reader.

The presence of siderophores (biologically produced organic molecules capable of binding Fe(III) with high affinity) was assayed using a colorimetric assay based on the dye, chrome azurol S (Alexander and Zuberer, 1991). This dye forms a blue compound when coordinated with Fe(III), and so sequestration of Fe(III) from the dye complex

BGD
8, 6345–6382, 2011

by siderophores causes a decrease in the blue color. To remove interference from dissolved Fe(III) in the water samples, it was necessary to dilute samples 10 fold and increase the $FeCl_3$ concentration in the dye reagent to 250 µm. Deferoxamine mesylate (Sigma-Aldrich) was used as a standard.

Dissolved CH_4 and CO_2 were analyzed in non-acidified water samples. Stoppered 25 ml flasks were flushed with N_2 gas for 1 min, 1.0 ml soil pore water was injected by syringe, allowed to equilibrate at 22 °C overnight, and the headspace was sampled by syringe and analyzed by gas chromatography (Model 8610C with methanizer and flame ionization detector, SRI Instruments, Torrance, CA). Original dissolved gas concentrations were calculated from the headspace concentrations and Henry's law constants for the two gases.

2.4 Microbial activity and biomass

On three dates in 2009, soil cores were collected to a depth of 15 cm using a serrated knife, sealed in two layers of Bitran specimen bags, and frozen. Cores were weighed, and the volume of the frozen cores wrapped tightly in plastic wrap was determined by displacement of water. Subsamples of these soils (~25 g wet weight) were placed in sealed mason jars with septa installed in the lids, and allowed to thaw under N_2 gas overnight at 4^oC. The following day the jars were again flushed with N_2 gas to remove accumulated gases, syringe samples were taken at 6 and 24 h after this point, and analyzed by gas chromatography as described above. Other subsamples from these cores were subjected to chloroform fumigation-extraction for indices of microbial biomass C and N. Organic C and ninhydrin-reactive N in these extracts were measured as described above. Subsamples were also used in proteolysis measurements: soils (~5 g wet weight) were placed in tubes with 20 mL sodium acetate buffer (50 mm, pH 5.0) with 1 % bovine serum albumin (BSA) as a protein source, and 0.4 ml toluene to inhibit amino acid uptake. Samples and soil-free controls were incubated at 6 °C on a shaker for 16h. Samples were removed, remaining BSA was precipitated by heating at 95 °C for 10 min, and released amino acids were measured using the ninhydrin

BGD
8, 6345–6382, 2011

assay. Microbial biomass and proteolytic rates were also measured on soils collected in July 2008.

Seasonal changes in solid-phase Fe was determined by extracting frozen soils in 1 N H_2SO_4 for 24 h. The resulting extracts were diluted and assayed for Fe^{2+} and Fe^{3+} as described above.

A measure of N availability to plants was obtained by burying at a depth of 5 cm nylon bags with 10 g mixed bed ion exchange resins. The resin was rinsed with copious amounts of distilled water before placing in the field, and replicate resin bags stored at 4^oC served as controls. Resin bags were placed in the soil at the beginning of the July and collected in mid-August. Resin bags were extracted in 2M KCl, analyzed for NH_4^+ and NO_3^-, and values from control bags were subtracted. This method was used in 2007 (before the flooding treatment) and again in 2009. Resin bags were installed near the same permanent plots referred to above (three high and three low locations in each transect).

2.5 Statistical analysis

Specific statistical tests used for each data set are described in the results section. These included general linear models (GLM), analysis of variance (ANOVA), analysis of covariance (ANCOVA) as well as simple regression and correlation analysis. Systat (v. 12.0) was used for all analyses. P values less than 0.05 are considered significant, while $0.1 > P \geq 0.05$ are referred to as marginally significant.

3 Results

3.1 Flooding treatment

The experimental basin increases in polygonization from south to north. This can be seen as a widening range of elevations from south to central to north treatment areas

BGD
8, 6345–6382, 2011

(Fig. 1a). The north includes areas with elevations as low as 1.5 m, but these were omitted from the analysis so that a comparable range of elevations would exist between the flooded and reference areas. At any given time, water table height was a function of microtopography, with lower elevation areas experiencing larger water table heights and a disproportionately large effect of the flooding treatment (Fig. 1a). The effects of elevation ($F = 103.8$, $P = 0.000$), treatment area (N, C and S) ($F = 38.0$, $P = 0.000$) and the interaction ($F = 29.0$, $P = 0.000$) were all highly significant for this ANCOVA ($n = 403$, $R^2 = 0.736$).

In 2008, the flooding treatment initially raised the average water table height by 8.6 cm relative to non-flooded areas, reaching a maximum differential of 15.3 cm by the end of summer (data not shown) (Olivas et al., 2010). In 2009, the flooding treatment initially achieved an average water table height 4.0 cm higher than the non-flooded treatment areas, reaching a maximum differential of 22.5 cm at the end of July (Fig. 1b). (Late in the summer of 2009, water was pumped into the south region to create an intermediate water table treatment; however, none of the data presented here were affected by this treatment). The wetter soils conducted heat more efficiently, leading to warmer temperatures in mid-summer (Fig. 1c). Averaged across all dates, temperatures measured in the flooding treatment were 1.0 °C higher than in the unflooded treatments.

3.2 Soil electrochemistry

Soil ORP and pH were both controlled by water table height (Fig. 2a, b), with more reducing and less acidic conditions in wetter areas. Accordingly, in an ANCOVA ORP was positively correlated ($R^2 = 0.287$, $F = 68.2$, $P < 0.001$) and pH negatively correlated ($R^2 = 0.388$, $F = 118.6$, $P < 0.001$) with elevation, and for any given elevation, pH was higher ($F = 100.1$, $P < 0.001$) and ORP lower ($F = 71.9$, $P < 0.001$) in the flooding treatment (Fig. 2c and d). The negative correlation between pH and ORP was highly significant (Table 1).

The seasonal pattern of ORP followed that of water table, becoming more oxic as water levels dropped (Fig. 3a, b); but pH increased during the early growing season,

BGD
8, 6345–6382, 2011

particularly in low elevation classes (Fig. 3c, d), corresponding to a period where reduction of solid phase Fe minerals was observed (Lipson et al., 2010), see Sect. 3.4 below.

Conditions in the flooded treatment were generally anoxic at 5 cm depth or shallower throughout the measurement period (Table 2). In the unflooded areas conditions generally became oxic in the upper 5 cm by late July, as the water table had also dropped below 5 cm depth by this time (Fig. 1b). The effect of flooding on the oxycline depth was highly significant for the spatially-intensive 22–23 July data set (Kruskal-Wallis test $P < 0.001$). In the GLM analysis of this data (dfe = 120), elevation ($F = 48.0$, $P < 0.001$) and flooding ($F = 54.8$, $P < 0.001$) were also highly significant. For the less spatially-intensive seasonal sampling, the flooding effect was significant in a two-way ANOVA with date and flooding as categorical factors ($P = 0.016$).

Trends in pH, ORP and DO disappeared or reversed in the year following the water manipulation (2010). Before the flooding treatment was initiated and after it ceased, soil pH was slightly lower in the north section of the experimental basin (Fig. 4). Likewise, trends observed in ORP and DO during the flooding treatment reversed in 2010 (grand means for 2010 at 10 cm depth: ORP in north = 247 ± 10 mV, south = 166 ± 1.6 mV; DO in north = 3.81 ± 0.44 mg l^{-1}, south = 2.15 ± 0.04 mg l^{-1}).

3.3 Soil water chemistry

Soil pore water concentrations (from 0–5 cm depth) of aromatic compounds (A260), DOC, Fe(III), NH_4^+, amino-N and PO_4, all declined exponentially throughout the season (Fig. 5). Therefore data were log-transformed to linearize this trend, and ANCOVA were run using date as a continuous variable and topography and flooding as factors (no significant interactions with date were found in these models). In the case of PO_4, the three-way ANOVA (with date coded categorically) had a significantly lower corrected Aikake information criterion (AIC_c) than the ANCOVA, and so these results are reported instead of the ANCOVA (Table 3). Significance of effects did not vary between the two model types, with one exception (see results for NH_4^+ below). Because the effects of

BGD
8, 6345–6382, 2011

flooding and topography were generally independent of date, to simplify presentation for most variables only the grand means of each treatment category are shown in Fig. 6. In the case of NH_4^+, certain dates appeared to have a disproportionate effect, and so the seasonal patterns for flooded and unfloooded treatments are shown (Fig. 6h).

A260, DOC, and Fe(III) followed similar trends (Fig. 6a–c) and were highly correlated (Table 1). All were significantly higher in low elevation areas (Table 3). A260 was significantly higher in the flooding treatment; Fe(III) was significantly higher in low elevation areas of the flooded treatment (topography × flooding interaction). The effect of flooding on DOC was significant ($P = 0.02$), and while the response appeared to be driven by low elevation areas (Fig. 6b), the topography × flooding interaction was marginal ($P = 0.098$).

For two dates later in the season, soil water samples were also collected from deeper in the profile (5–15 cm). On these dates, dissolved Fe(III) concentrations and A260 values were significantly higher at depth, by factors of 2.65 and 2.36, respectively (data not shown). Mean DOC concentrations were only 1.33 times higher at depth, and this difference was not statistically significant (data not shown).

Trends in A260 and Fe(III) reversed in the following year, after the flooding treatment had ceased (grand means for 2010: Fe(III) in north = 74.9 ± 13.0 µm, south = 183.7 ± 23.6 µm; A260 in north = 0.232 ± 0.071 AU, south = 0.394 ± 0.071 AU).

Soil pore water samples were assayed for the presence of siderophores on a single day (8 July) in 2009 (Fig. 6d). In a two-way ANOVA, the concentration of siderophores was much higher in low elevation areas ($F = 38.9$, $P < 0.001$) and there was no significant effect of flooding. The same pattern held in 2010 (data not shown), and including data for both 2009 and 2010, siderophore concentrations were highly positively correlated with total dissolved Fe (correlation coefficient $r = 0.931$, $n = 44$) and A260 ($r = 0.862$, $n = 33$), and negatively correlated with ORP ($r = 0.751$, $n = 26$).

PO_4 was significantly higher in the flooded treatment and the effect of topography was only marginally significant (Fig. 6e, Table 3). There was no significant effect of topography or flooding on amino-N in soil pore water (Fig. 6f, Table 3). Neither were

BGD
8, 6345–6382, 2011

there consistent effects of flooding or topography on NH_4^+ (Table 3). The higher grand means for NH_4^+ concentrations in the flooding treatment (Fig. 6g) were due to higher values early in the summer (Fig. 6h), leading to a significant date × flooding interaction in the three-way ANOVA with date coded categorically ($P = 0.031$). NO_3^- concentrations were below detection limits (~5 µm) in the majority of water samples, and the mean NO_3^- concentrations for flooded and unflooded treatments were nearly identical (4.9 vs. 5.1 µm, respectively; data not shown).

Dissolved CH_4 and CO_2 concentrations were correlated with each other and with A260, DOC and Fe(III) (Table 1). Like most of the other soil water variables, dissolved CO_2 also declined throughout the season (Fig. 7a). Dissolved CH_4 followed a different seasonal pattern, peaking in mid-summer (Fig. 7b). Because of this, the three-way ANOVA of dissolved CH_4 with date coded categorically had significantly lower AIC_c than the ANCOVA with date coded as a continuous variable (Table 3). At a depth of 0–5 cm, both CO_2 and CH_4 were found in significantly higher concentrations in topographically low areas (Fig. 7a, b). Across all dates, dissolved CO_2 concentrations were significantly lower in high elevation, flooded areas (Topo X Flood interaction in Table 3, Fig. 7a); the similar trend for CH_4 (Fig. 7b) was marginally significant ($P = 0.087$, Table 3).

On one day towards the end of summer (1 August 2009), higher dissolved CO_2 and CH_4 concentrations were observed in low elevation areas of the flooding treatment. This led to marginally significant date × flooding interactions ($P = 0.067$ and 0.063 for CO_2 and CH_4). This change in the effect of the flooding treatment coincided with a period when water tables in the control areas were rapidly dropping to near-minimum levels (Fig. 1b); the flooding treatment appears to have extended conditions favorable for CH_4 and CO_2 accumulation later into the season. On this day only (by happenstance), water samples were also collected from 5–15 cm depth at the same locations and analyzed for dissolved CO_2 and CH_4 (Fig. 7c, d). A three-way ANOVA was run using topography, depth and flooding as factors (dfe = 28). For CH_4, concentrations were significantly higher at depth ($F = 16.1$, $P < 0.001$), in low elevation areas ($F = 22.9$, $P < 0.001$)

BGD
8, 6345–6382, 2011

and in the flooding treatment ($F = 11.1$, $P = 0.002$), and the topography × flooding interaction was also significant ($F = 5.3$, $P = 0.029$), indicating that the flooding response was driven by low elevation areas. For CO_2, the effects of flooding ($F = 8.2$, $P = 0.008$), topography ($F = 31.7$, $P < 0.001$) and depth ($F = 32.7$, $P < 0.001$) were significant, as was the topography × flooding interaction ($F = 9.4$, $P = 0.005$), indicating the differential effect of flooding on high vs. low areas, and the depth × topography interaction ($F = 5.5$, $P = 0.027$), stemming from the steeper depth gradient in topographically high areas. (A steeper gradient along the profile implies more rapid diffusion in high elevation areas.) Ratios of dissolved CO_2:CH_4 ranged from 46 (at 5–15 cm in low areas of flooding treatment) to 572 (0–5 cm in high areas of unflooded treatment).

Many soil chemistry variables responded in concert to natural and experimental changes water table height, as seen in the intercorrelations of A260, Fe(III), CO_2, and CH_4; their positive correlations with pH and their negative correlations with ORP (Table 1). Furthermore, the logarithm of dissolved Fe(III) was positively correlated with the height of the water table ($r = 0.369$, $n = 119$, $P < 0.001$), in a regression that incorporated both seasonal and spatial variation.

3.4 Microbial activity and biomass

Consistent with the effects of flooding and microtopography on ORP and DO shown above, anaerobic microbial processes also responded to natural and experimental variations in water table height (Fig. 8). Potential CO_2 and CH_4 production rates were measured in anaerobic laboratory incubations on three dates, and effects were tested using a three-way ANOVA with date, topography and flooding as factors. CO_2 production rates in anaerobic incubations were highest on the first date ($P = 0.038$), and higher in the flooding treatment ($P = 0.012$), apparently due to higher rates in high elevation areas (although the topography × flooding interaction was not significant: $P = 0.168$). The topographic effect on anaerobic CO_2 production was only marginally significant ($P = 0.079$, Fig. 8a). CH_4 production rates in these incubations were higher in low elevation areas and in the flooding treatment ($P < 0.001$ for both; date and interactions not

BGD
8, 6345–6382, 2011

significant, Fig. 8b). The CO_2:CH_4 ratios evolved in incubations were similar to those dissolved in soil pore water, ranging from 42 (low areas of flooded treatments) to 890 (high areas of unflooded treatments).

Dissimilatory Fe(III) reduction over the course of the summer was monitored as changes in the reduction state of Fe-bearing minerals in the soil. Acid-extractable Fe(III) declined throughout the season as Fe(II) increased, indicating net Fe reduction (Fig. 8c). Fe(II) was significantly higher in low areas of the landscape ($P = 0.015$). Flooding effects were not statistically significant. Seasonal Fe reduction rates calculated from either the increase in Fe(II) or the decrease in Fe(III) in the acid soluble fraction were greater in low elevation areas (high: 6.4–27.4 m mole Fe m^{-2} d^{-1}; low: 28.0–36.4 m mole Fe m^{-2} d^{-1}, with low and high ranges based on ΔFe(II) and ΔFe(III), respectively).

In contrast to these measures of anaerobic activity, more general measures of microbial biomass showed more subtle responses. Microbial Biomass C, measured by fumigation-extraction, showed no significant effects of flooding, topography or date (Fig. 9a). Microbial biomass N (measured as ninhydrin-active N released by fumigation extraction) showed marginally significant effects driven by lower means in flooded, low-elevation areas in 2009 (Fig. 9b). In a GLM analysis (dfe = 44), date was significant ($F = 9.106$, $P = 0.000$), the flooding effect ($F = 3.252$, $P = 0.078$) and the topography × flooding interaction ($F = 3.215$, $P = 0.080$) were marginally significant, and the direct topography effect was not significant ($F = 1.687$, $P = 0.201$).

Soil protease activity varied by date ($P = 0.016$), but flooding and topographic effects were not significant (Fig. 9c). In contrast, N availability integrated over the summer appeared to respond to water table height: N captured by buried resin bags was higher in low elevation areas during the pre-flooding year (2007) and higher in the flooding treatment in 2009 (Fig. 9d). In the three-way ANOVA comparing year, treatment area, and topography (dfe = 30), topography ($F = 4.421$, $P = 0.044$) and the year × transect interaction ($F = 5.218$, $P = 0.030$) were significant.

BGD
8, 6345–6382, 2011

4 Discussion

Being a relatively flat area with drainage blocked by permafrost and a climate with generally low evaporative demand, this ecosystem is subject to regular flooding from snow melt. Therefore, experimental flooding mainly accentuated the normally occurring responses to seasonal and spatial variation in water table height. Microtopography arising from ice wedge polygons controls spatial variation in water table height, leading to sharp contrasts in soil chemistry and microbiology over short spatial scales. The effects of the flooding treatment recovered quickly after the water table manipulation ended: during the flooding treatment ORP was lower and pH, Fe(III) and A260 were higher in the north (flooded) section compared to the south section, but these trends reversed in 2010 after the flooding treatment had ended. In the absence of the experimental manipulation, the less polygonized southern end of the basin was more reducing, on average, than the more polygonized northern section. Increased polygonization leads to a greater abundance of elevated, oxic areas within the landscape, which appears to raise the overall average ORP of the landscape.

Many of the observed effects of natural and experimental variation in water table height can be attributed to lower diffusion rates of gases in wet soils (Fig. 10). Inundated areas become anoxic, and the microbial communities appear to respond by producing organic ligands that solubilize Fe(III). The process of solubilizing and reducing Fe(III) (as well as other alternative e^- acceptors) consumes protons, leading to higher pH (Reddy and DeLaune, 2008). Conversely, protons are released and pH is lowered under oxidizing conditions; this was seen dramatically in 2007 (Fig. 4), an exceptionally dry year in which water table height dropped to much lower levels then in other years of the study (Olivas et al., 2010). Flooded, anoxic conditions also promote the growth and activity of methanogens, and lower diffusion rates can also trap more CH_4 in the soil. However, the increased availability of Fe(III) could competitively inhibit methane production (Roden and Wetzel, 1996; Bond and Lovley, 2002; Küsel et al., 2008; Jerman et al., 2009), weakening these effects (dotted flat arrow in lower left, Fig. 10). High

BGD
8, 6345–6382, 2011

water tables also slow diffusion of CO_2 out of the soil, leading to higher concentrations in lower, wetter areas. It is also possible that microtopographic patterns of plant growth and litter accumulation contribute to higher dissolved CO_2 concentrations in polygon centers (dotted arrow in upper right, Fig. 10) (Zona et al., 2011a).

The inference that microbes solubilize Fe(III) in response to anoxia is based on (1) the surprisingly high concentrations of Fe(III) in soil pore water, given only moderately acidic conditions, best explained by the presence of organic chelating agents; (2) the high concentrations of siderophores in pore water of low, anoxic areas; and (3) the strong correlations among soluble Fe, siderophores, the UV absorbance of soil pore water (A260) and ORP. Aromatic compounds, including several classes of siderophores (Drechsel and Jung, 1998), strongly absorb UV wavelengths. The presence of Fe can also enhance the UV absorbance of solutions (Weishaar et al., 2003), though the correlations of A260 with DOC and siderophores show that the relationship between Fe(III) and A260 was not produced entirely by this effect.

It has already been established that the process of Fe(III) reduction is important in this ecosystem (Lipson et al., 2010). This is expressed in the current study as the high availability of soluble Fe(III), the relationship between redox conditions and pH (indicating that proton-consuming reactions such as Fe(III) reduction take place where reducing conditions predominate), and the seasonal changes in the reduction state of solid-phase Fe minerals. The high ratios of CO_2:CH_4 dissolved in soil pore water and produced in anaerobic laboratory incubations also indicate an ecosystem with an abundance of alternative e- acceptors for anaerobic respiration (Updegraff et al., 1995; van Hulzen et al., 1999; Keller and Bridgham, 2007; Keller et al., 2009). In the absence of alternative e^- acceptors, equimolar concentrations of CO_2 and CH_4 would be produced (i.e., a ratio of one), whereas values ranging from 42 to 890 were observed in incubations and dissolved in soil pore water. Hence, even in the most anoxic areas of the landscape, methanogenesis still constituted a minor fraction of metabolic e^- flow (at least for the surface layers studied here). This explains why reported CH_4 fluxes from this landscape (24.6 mg CH_4 m^{-2} d^{-1}) (Zona et al., 2009) are near the low end for

BGD
8, 6345–6382, 2011

those reported in the Arctic (Blodau, 2002; Wagner et al., 2003). And so in terms of climate change, the potential for increased methane production from ecosystems such as the DTLB studied here could be limited by the high availability of Fe(III).

The results of this and a previous study (Lipson et al., 2010) indicate that microbial communities in much of this landscape are dominated by facultative and/or strict anaerobes. It was mainly in high elevation areas (e.g., polygon rims), where conditions were normally oxic near the surface for most of the year, where the potential for anaerobic respiration responded to the flooding treatment (Fig. 8a), indicating that anaerobically-respiring microbes were already abundant in low areas of the landscape. Methanogens, being strict anaerobes that thrive in the most reducing conditions, responded more dramatically to the flooding treatment and showed a marked preference for low elevation areas, where the risk of exposure to O_2 is lower (Fig. 8b). This landscape pattern has been noted in other studies (Wagner et al., 2003; Strack and Waddington, 2007). There were only the subtlest of hints that flooding might create suboptimal conditions for microbial activity: lower dissolved CO_2 concentrations in flooded, topographically high areas could have been caused by a depression of respiration due to suboxic conditions (Fig. 7a). Microbial biomass C was not impacted by flooding, though one could argue that the statistically weak decrease in microbial biomass N in low elevation areas of the flooding treatment represented a negative microbial response to flooding. However, there was no consistent trend toward lower microbial biomass C or N in lower elevation areas, indicating that anoxic conditions do not generally limit the biomass of the local microbial community. Flooding experiments in northern peat soils have often produced insignificant or relatively minor effects on ecosystem respiration (Updegraff et al., 2001; Chivers et al., 2009; Huemmrich et al., 2010), while lowering water table tends to have more dramatic effects (Oechel et al., 1998; Strack et al., 2006; Strack and Waddington, 2007; Sommerkorn, 2008). This dichotomy is understandable given the tendency of these ecosystems toward waterlogged, suboxic conditions. Increases in soil CO_2 fluxes with lowered water tables is generally attributed to increased O_2 availability (Billings et al., 1982; Sommerkorn,

BGD
8, 6345–6382, 2011

2008; Olivas et al., 2010). While O_2 certainly plays a major role, the impressive capacity for anaerobic respiration of some peat soils should not be overlooked. At our study site, the flooded (north) treatment area was submerged under water for nearly the entire 2008 growing season, and yet chamber-based measurements of ecosystem respiration were only 23 % less than those measured in the control area, where the water table was generally below the surface (Olivas et al., 2010). Moreover, landscape scale measurements of net ecosystem CO_2 exchange and estimation of ecosystem respiration from eddy covariance showed that the flooded area presented higher CO_2 loss with higher wind speed. The CO_2 produced by soil respiration and dissolved in the water probably diffused into the atmosphere with the rate of exchange increased at high wind speed not captured by chamber measurements (Zona et al., 2011b). Our observation in the current study of high dissolved CO_2 concentrations in low, wet areas suggests that the effects of soil water on diffusion rates of CO_2 should be considered when interpreting the effects of water table on measurements of ecosystem respiration.

The increased concentrations of P seen in the flooded treatment could be caused by redox-mediated release of P occluded in ferric hydroxides, as has been observed in other studies (Chambers and Odum, 1990; Shenker et al., 2005). The nutrient cycling effects might also be explained by the temperature/thaw depth aspect of the flooding treatment. The largest increases in nutrient concentrations were shortly after break up, before soil temperatures had warmed in response to the flooding treatment. The increases in N and P concentrations observed in the flooding treatments early in 2009 could have been partly caused by the release of labile substrates from permafrost due the increased thaw depth in 2008 (Shiklomanov et al., 2010). The increased N bound to buried resin bags could have also have been a result of increased soil temperatures in the current year leading to greater rates of N mineralization. In high Arctic regions of continuous permafrost, where thermokarsting is leading to expansion of flooded areas (Smith et al., 2005), warming and flooding could have a positive interactive effect on nutrient availability.

BGD
8, 6345–6382, 2011

The observed pulse of nutrients after snow melt is commonly reported in arctic, alpine and other cold ecosystems (Chapin et al., 1978; Zak et al., 1990; Brooks et al., 1998; Lipson et al., 1999; Edwards et al., 2006). Maximum thaw depths occur in late summer after plants have already begun to senesce (Olivas et al., 2010) and so nutrients made available from thawing of permafrost might not be accessible to plants until the following break up. The rapid decline after snow melt of dissolved nutrients probably represents rapid uptake by plants. This early season pulse has long been hypothesized to represent a major contribution to plant nutrient requirements in Arctic coastal tundra (Chapin et al., 1978), and such a pattern would help plants capitalize on nutrients mobilized from recently thawed permafrost.

5 Summary and conclusions

The flooding treatment produced two distinct suites of results: (1) elevated water table heights led to more reducing conditions, stimulating anaerobic processes such as Fe(III) reduction and methanogenesis; (2) Flooding stimulated N and P availability, possibly due to warmer temperatures and deeper active layer depths, though increased soluble P could also be explained by reduction of Fe minerals. This study also highlights the importance of ice wedge polygon-induced microtopography in shaping landscape patterns of soil chemistry and microbiology, and provides more evidence for the importance of dissimilatory Fe(III) reduction as a dominant process in this ecosystem.

Acknowledgements. The authors wish to thank Faustine Bernadac, Steve Hastings, Louis Brower and many others from BASC and CPS for logistical support, the UIC for access to their land, Maria Santos for assistance in the field, and Ling Han and Dominic Goria for assistance in laboratory analysis. The work was funded by NSF grants OPP-0421588 to W. C. O. and ARC-0808604 to D. A. L.

BGD
8, 6345–6382, 2011

References

Alexander, B. and Zuberer, D. A.: Use of chrome azurol S reagents to evaluate siderophore production by rhizosphere bacteria, Biol. Fert. Soil., 12, 39–45, 1991.

Analytical Methods Committee: Standardized general method for the determination of iron with 1,10-phenanthroline, Analyst, 103, 391–396, 1978.

Bartlett, R. J. and Ross, D. S.: Colorimetric determination of oxidizable carbon in acid soil solutions, Soil Sci. Soc. Am. J., 52, 1191–1192, 1988.

Billings, W. D. and Peterson, K. M.: Vegetational change and ice-wedge polygons through the thaw-lake cycle in arctic Alaska, Arctic Alpine Res., 12, 413–432, 1980.

Billings, W. D., Lukens, J. O., Mortensen, D. A., and Peterson, K. M.: Arctic tundra: A source or sink for atmospheric carbon dioxide in a changing environment?, Oecologia, 53, 7–11, 1982.

Blodau, C.: Carbon cycling in peatlands – A review of processes and controls, Environ. Rev., 10, 111–134, 2002.

Bloom, A. A., Palmer, P. I., Fraser, A., Reay, D. S., and Frankenberg, C.: Large-scale controls of methanogenesis inferred from methane and gravity spaceborne data, Science, 327, 322–325, 2010.

Bockheim, J., Hinkel, K., Eisner, W., and Dai, X.: Carbon pools and accumulation rates in an age-series of soils in drained thaw-lake basins, Arctic Alaska, Soil Sci. Soc. Am. J., 68, 697–704, 2004.

Bond, D. and Lovley, D.: Reduction of Fe(III)) oxide by methanogens in the presence and absence of extracellular quinones, Environ. Microbiol., 4, 115–124, 2002.

Brooks, P. D., Williams, M. W., and Schmidt, S. K.: Inorganic nitrogen and microbial biomass dynamics before and during spring snowmelt, Biogeochemistry, 43, 1–15, 1998.

Brown, J.: Tundra soils formed over ice wedges, northern Alaska, Soil Sci. Soc. Am. Proc., 31, 686–691, 1967.

Chambers, R. M. and Odum, W. E.: Porewater oxidation, dissolved phosphate and the iron curtain Iron-phosphorus relations in tidal freshwater marshes, Biogeochemistry, 10, 37–52, 1990.

Chapin, F. S., Barsdate, R. J., and Barèl, D.: Phosphorus cycling in Alaskan coastal tundra: a hypothesis for the regulation of nutrient cycling, Oikos, 31, 189–199, 1978.

BGD
8, 6345–6382, 2011

Chivers, M. R., Turetsky, M. R., Waddington, J. M., Harden, J. W., and McGuire, A. D.: Effects of experimental water table and temperature manipulations on ecosystem CO_2 fluxes in an Alaskan rich fen, Ecosystems, 12, 1329–1342, 2009.
Drechsel, H. and Jung, G.: Peptide Siderophores, J. Pept. Sci., 4, 147–181, 1998.
Edwards, K. A., McCulloch, J., Kershaw, G. P., and Jefferies, R. L.: Soil microbial and nutrient dynamics in a wet Arctic sedge meadow in late winter and early spring, Soil Biol. Biochem., 38, 2843–2851, 2006.
Hinkel, K. M., Eisner, W. R., Bockheim, J. G., Nelson, F. E., Peterson, K. M., and Dai, X.: Spatial extent, age, and carbon stocks in drained thaw lake basins on the Barrow Peninsula, Alaska, Arct. Antarct. Alp. Res., 35, 291–300, 2003.
Huemmrich, K. F., Kinoshita, G., Gamon, J. A., Houston, S., Kwon, H., and Oechel, W. C.: Tundra carbon balance under varying temperature and moisture regimes, J. Geophys. Res., 115, G00I02, doi:10.1029/2009JG001237, 2010.
IPCC: Summary for Policymakers, in: Climate Change 2007: The Physical Science Basis, Contribution of Working Group I to the Fourth Assessment Report of the Intergovernmental Panel on Climate Change, edited by: Solomon, S., Qin, D., Manning, M., Chen, Z., Marquis, M., Averyt, K. B., Tignor, M., and Miller, H. L., Cambridge University Press, Cambridge, UK and New York, NY, USA, 2007.
Jerman, V., Metje, M., Mandić-Mulec, I., and Frenzel, P.: Wetland restoration and methanogenesis: the activity of microbial populations and competition for substrates at different temperatures, Biogeosciences, 6, 1127–1138, doi:10.5194/bg-6-1127-2009, 2009.
Keller, J. K. and Bridgham, S. D.: Pathways of anaerobic carbon cycling across an ombrotrophic-minerotrophic peatland gradient, Limnol. Oceanogr., 52, 96–107, 2007.
Keller, J. K., Weisenhorn, P. B., and Megonigal, J.P.: Humic acids as electron acceptors in wetland decomposition, Soil Biol. Biochem., 41, 1518–1522, 2009.
Knorr, K. H. and Blodau, C.: Impact of experimental drought and rewetting on redox transformations and methanogenesis in mesocosms of a northern fen soil, Soil Biol. Biochem., 41, 1187–1198, 2009.
Kögel-Knabner, I., Amelung, W., Cao, Z., Fiedler, S., Frenzel, P., Jahn, R., Kalbitz, K., Kölbl, A., and Schloter, M.: Biogeochemistry of paddy soils, Geoderma, 157, 1–14, 2010.
Küsel, K., Blöthe, M., Schulz, D., Reiche, M., and Drake, H. L.: Microbial reduction of iron and porewater biogeochemistry in acidic peatlands, Biogeosciences, 5, 1537–1549, doi:10.5194/bg-5-1537-2008, 2008.

BGD
8, 6345–6382, 2011

Kujala, K., Seppälä, M., and Holappa, T.: Physical properties of peat and palsa formation, Cold Reg. Sci. Technol., 52, 408–414, 2008.
Kuo, S.: Phosphorus, in: Methods of Soil Analysis, Part 3: Chemical Methods, edited by: Sparks, D. L., American Society of Agronomy, Madison, WI, 869–920, 1996.
Lipson, D. A., Schmidt, S. K., and Monson, R. K.: Links between microbial population dynamics and N availability in an alpine ecosystem, Ecology, 80, 1623–1631, 1999.
Lipson, D. A., Jha, M., Raab, T. K., and Oechel, W. C.: Reduction of iron (III) and humic substances plays a major role in anaerobic respiration in an Arctic peat soil, J. Geophys. Res.-Biogeo., 115, G00I06, doi:10.1029/2009JG001147, 2010.
O'Donnell, J. A., Romanovsky, V. E., Harden, J. W., and McGuire, A. D.: The effect of moisture content on the thermal conductivity of moss and organic soil horizons from black spruce ecosystems in interior Alaska, Soil Sci., 174, 646–651, 2009.
Oechel, W. C., Vourlitis, G. L., Hastings, S. J., Ault, R. P., and Bryant, P.: The effects of water table manipulation and elevated temperature on the net CO_2 flux of wet sedge tundra ecosystems, Global Change Biol., 4, 77–90, 1998.
Olivas, P. C., Oberbauer, S. F., Tweedie, C. E., Oechel, W. C., and Kuchy, A.: Responses of CO_2 flux components of Alaskan Coastal Plain tundra to shifts in water table, J. Geophys. Res., 115, G00I05, doi:10.1029/2009JG001254, 2010.
Reddy, K. R. and DeLaune, R. D.: Biogeochemistry of wetlands: science and applications, CRC Press, Boca Raton, FL, 2008.
Rhew, R. C., Teh, Y. A., and Abel, T.: Methyl halide and methane fluxes in the northern Alaskan coastal tundra, J. Geophys. Res., 112, G02009, doi:10.1029/2006JG000314, 2007.
Roden, E. E. and Wetzel, R. G.: Organic carbon oxidation and suppression of methane production by microbial Fe(III)oxide reduction in vegetated and unvegetated freshwater wetland sediments, Limnol. Oceanogr., 41, 1733–1748, 1996.
Schuur, E. A. G., Bockheim, J., Canadell, J. G., Euskirchen, E., Field, C. B., Goryachkin, S. V., Hagemann, S., Kuhry, P., Lafleur, P. M., Lee, H., Mazhitova, G., Nelson, F. E., Rinke, A., Romanovsky, V. E., Shiklomanov, N., Tarnocai, C., Venevsky, S., Vogel, J. G., and Zimov, S. A.: Vulnerability of permafrost carbon to climate change: implications for the global carbon cycle, Bioscience, 58, 701–714, 2008.
Shenker, M., Seitelbach, S., Brand, S., Haim, A., and Litaor, M. I.: Redox reactions and phosphorus release in re-flooded soils of an altered wetland, Eur. J. Soil Sci., 56, 515–525, 2005.

BGD
8, 6345–6382, 2011

Shiklomanov, N. I., Streletskiy, D. A., Nelson, F. E., Hollister, R. D., Romanovsky, V. E., Tweedie, C. E., Bockheim, J. G., and Brown, J.: Decadal variations of active-layer thickness in moisture-controlled landscapes, Barrow, Alaska, J. Geophys. Res., 115, G00I04, doi:10.1029/2009JG001248, 2010.

Smith, L. C., Sheng, Y., MacDonald, G. M., and Hinzman, L. D.: Disappearing Arctic lakes, Science, 308, 1429, 2005.

Sommerkorn, M.: Micro-topographic patterns unravel controls of soil water and temperature on soil respiration in three Siberian tundra systems, Soil Biol. Biochem., 40, 1792–1802, 2008.

Strack, M. and Waddington, J.: Response of peatland carbon dioxide and methane fluxes to a water table drawdown experiment, Global Biogeochem. Cy., 21, GB1007, doi:10.1029/2006GB002715, 2007.

Strack, M., Waddington, J., Rochefort, L., and Tuittila, E.: Response of vegetation and net ecosystem carbon dioxide exchange at different peatland microforms following water table drawdown, J. Geophys. Res.-Biogeo., 111(G2), G02006, doi:10.1029/2005JG000145, 2006.

Tarnocai, C., Canadell, J. G., Schuur, E. A. G., Kuhry, P., Mazhitova, G., and Zimov, S.: Soil organic carbon pools in the northern circumpolar permafrost region, Global Biogeochem. Cy., 23, GB2023, doi:2010.1029/2008GB003327, 2009.

Updegraff, K., Pastor, J., Bridgham, S. D., and Johnston, C. A.: Environmental and substrate controls over carbon and nitrogen mineralization in northern wetlands, Ecol. Appl., 5, 151–163, 1995.

Updegraff, K., Bridgham, S. D., Pastor, J., Weishampel, P., and Harth, C.: Response of CO_2 and CH_4 Emissions From Peatlands to Warming And Water Table Manipulation, Ecol. Appl., 11, 311–326, 2001.

van Hulzen, J. B., Segersa, R., van Bodegoma, P. M., and Leffelaar, P. A.: Temperature effects on soil methane production: an explanation for observed variability, Soil Biol. Biochem., 31, 1919–1929, 1999.

von Fischer, J. C., Rhew, R. C., Ames, G. M., Fosdick, B. K., and von Fischer, P. E.: Vegetation height and other controls of spatial variability in methane emissions from the Arctic coastal tundra at Barrow, Alaska, J. Geophys. Res., 115, G00I03, doi:10.1029/2009JG001283, 2010.

Wagner, D., Kobabe, S., Pfeiffer, E.-M., and Hubberten, H.-W.: Microbial controls on methane fluxes from a polygonal tundra of the Lena Delta, Siberia, Permafrost Periglac. Process., 14, 173–185, 2003.

BGD
8, 6345–6382, 2011

Weishaar, J. L., Aiken, G. R., Bergamaschi, B., Fram, M. S., Fujii, R., and Mopper, K.: Evaluation of specific ultraviolet absorbance as an indicator of the chemical composition and reactivity of dissolved organic carbon, Environ. Sci. Technol., 37, 4702–4708, 2003.

Yavitt, J. B. and Seidman-Zager, M.: Methanogenic Conditions in Northern Peat Soils, Geomicrobiol. J., 23, 119–127, 2006.

Zak, D. R., Groffman, P. M., Pregitzer, K. S., Christensen, S., and Tiedje, J. T.: The vernal dam: plant-microbe competition for nitrogen in northern hardwood forests, Ecology, 71, 651–656, 1990.

Zona, D., Oechel, W. C., Kochendorfer, J., Paw U, K. T., Salyuk, A. N., Olivas, P. C., Oberbauer, S. F., and Lipson, D. A.: Methane fluxes during the initiation of a large-scale water table manipulation experiment in the Alaskan Arctic tundra, Global Biogeochem. Cy., 23, GB2013, doi:2010.1029/2009GB003487, 2009.

Zona, D., Lipson, D., Zulueta, R., Oberbauer, S., and Oechel, W.: Micro-topographic controls on ecosystem respiration in the Arctic tundra, J. Geophys. Res., doi:10.1029/2009JG001241, in press, 2011a.

Zona, D., Lipson, D. A., Barott, K., Paw-U, K. T., Oberbauer, S. F., Olivas, P., Hastings, S., Hinzman, L. D., and Oechel, W. C.: Inundation increases respiration loss from the Arctic tundra, Global Biogeochem. Cy., in revision, 2011b.

BGD

8, 6345–6382, 2011

Table 1. Correlations among dissolved species in soil water and electrochemical measurements. Upper diagonal shows correlation coefficients (those significant by Bonferroni test in bold). Lower diagonal shows sample size for each correlation.

	Fe3	A260	DOC	$logCH_4$	$logCO_2$	pH	ORP
Fe3		**0.824**	**0.702**	**0.361**	**0.561**	**0.49**	**−0.378**
A260	126		**0.79**	**0.401**	**0.593**	**0.538**	**−0.471**
DOC	102	102		0.292	**0.545**	0.253	**−0.593**
$logCH_4$	73	73	51		**0.79**	**0.505**	**−0.46**
$logCO_2$	73	73	51	73		**0.602**	**−0.553**
pH	126	126	102	73	73		**−0.583**
ORP	90	90	68	55	55	720	

BGD
8, 6345–6382, 2011

Table 2. Oxycline depth index. Values of 0–5 indicate the depth in cm at which dissolved O_2 dropped to near-anoxic levels. Value of 6 and 7 are non-parametric indicators of suboxic and oxic conditions, respectively, at 5 cm depth.

	Flooded	Unflooded
22 Jul–23 Jul intensive sampling		
median	3	7
mean	3.61	6.63
se	0.33	0.09
n	49	75
Seasonal sampling		
29 Jun 2009	4.17 (0.91)	4.17 (0.75)
15 Jul 2009	3.83 (1.45)	4.93 (0.62)
24 Jul 2009	5 (1.22)	7 (0)
29 Jul 2009	4.17 (1.28)	6.67 (0.26)

BGD
8, 6345–6382, 2011

Table 3. Statistical tests (F-statistic and p-values) on log-transformed water chemistry data (0–5 cm depth). For all but two variables, ANCOVA models were used with date as a continuous variable and flooding treatment and topography as categorical effects. For PO_4 and CH_4, the AIC_c of the three-way ANOVA models were significantly lower than the ANCOVA, and so ANOVA were used, with date coded categorically. No interactions with date were significant ($P < 0.05$) in any model. Topo = topographic effect, dfe = degrees of freedom in error.

		Date	Topo	Flooding	Topo × Flood	dfe
Fe(III)	F	26.127	92.994	0.243	8.345	121
	P	0	0	0.623	0.005	
A260	F	138.776	43.739	18.416	4.465	118
	P	0	0	0	0.037	
DOC	F	92.922	15.874	5.475	2.79	108
	P	0	0	0.021	0.098	
NH_4	F	28.781	0.03	1.827	0.002	120
	P	0	0.864	0.179	0.96	
Amino-N	F	46.849	1.781	0.005	1.009	121
	P	0	0.185	0.943	0.317	
PO_4	F	248.906	1.637	5.551	1.296	120
	P	0	0.203	0.02	0.257	
CO_2	F	13.634	80.015	0.265	5.833	66
	P	0	0	0.609	0.019	
CH_4	F	26.566	98.053	0.19	3.046	55
	P	0	0	0.664	0.087	

BGD
8, 6345–6382, 2011

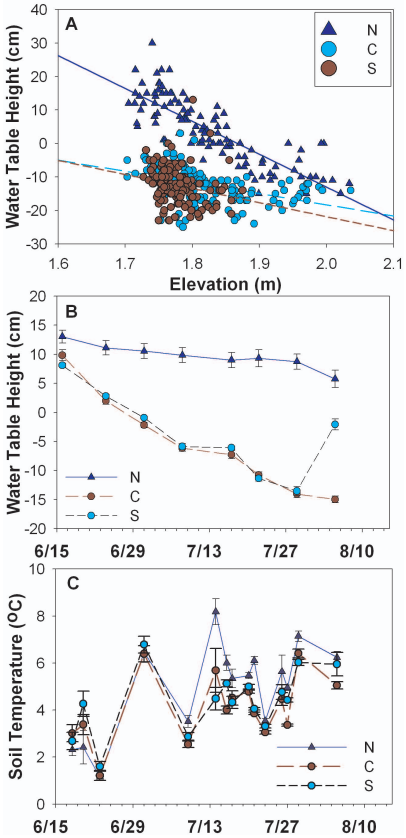

Fig. 1. (A) The relationship between water table depth and elevation, and the effects of flooding the North transect (N). Data is shown for 21–29 July 2009. Points with elevation below 1.7 m were omitted, as this elevation class existed only in the North transect. **(B)** Seasonal changes in water table height in the three treatment areas. **(C)** Soil temperature at 10 cm (measurements associated with pH and ORP measurements across each transect, generally made between 10:00 a.m. and 06:00 p.m.).

BGD
8, 6345–6382, 2011

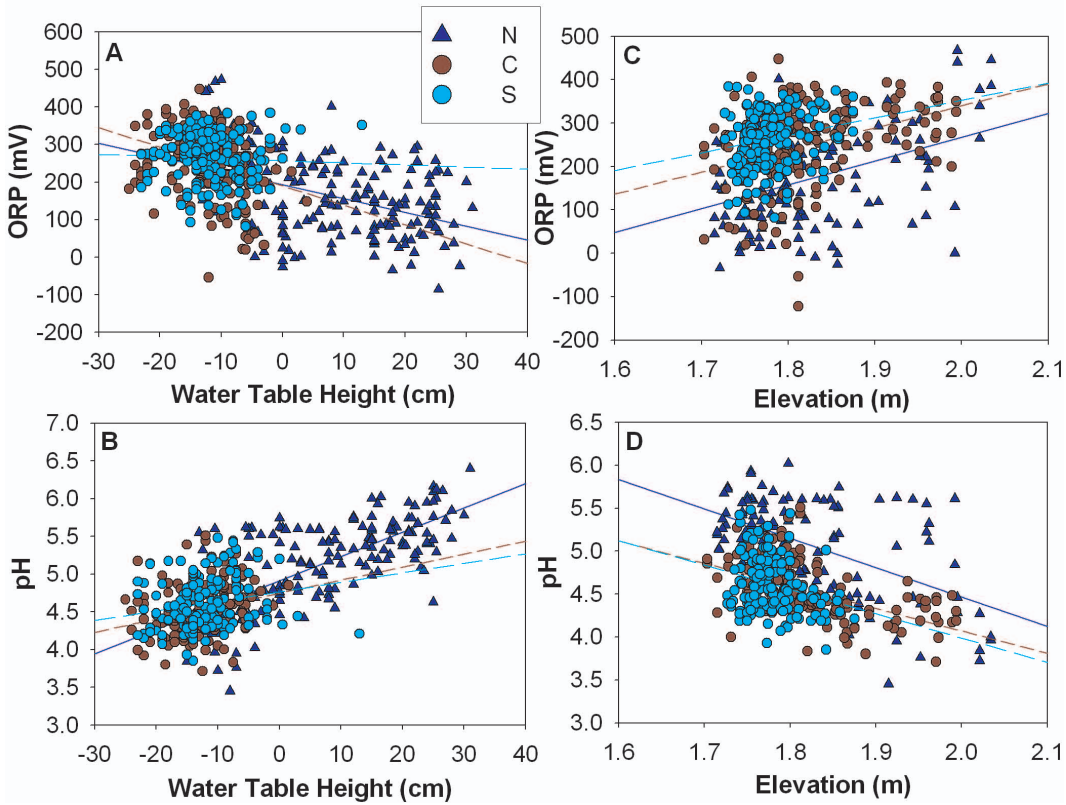

Fig. 2. Relationships of oxidation-reduction potential (ORP) and pH with water table height and elevation. **(A)** ORP vs. water table; **(B)** pH vs. water table; **(C)** ORP vs. elevation; **(D)** pH vs. elevation. Data is shown for 17–29 July 2009. The North transect (N) was experimentally flooded. For the plots showing relationships with elevation, data were omitted for elevations <1.7 m, which only occurred in the North transect. ORP values are relative to a Ag/AgCl reference electrode.

BGD
8, 6345–6382, 2011

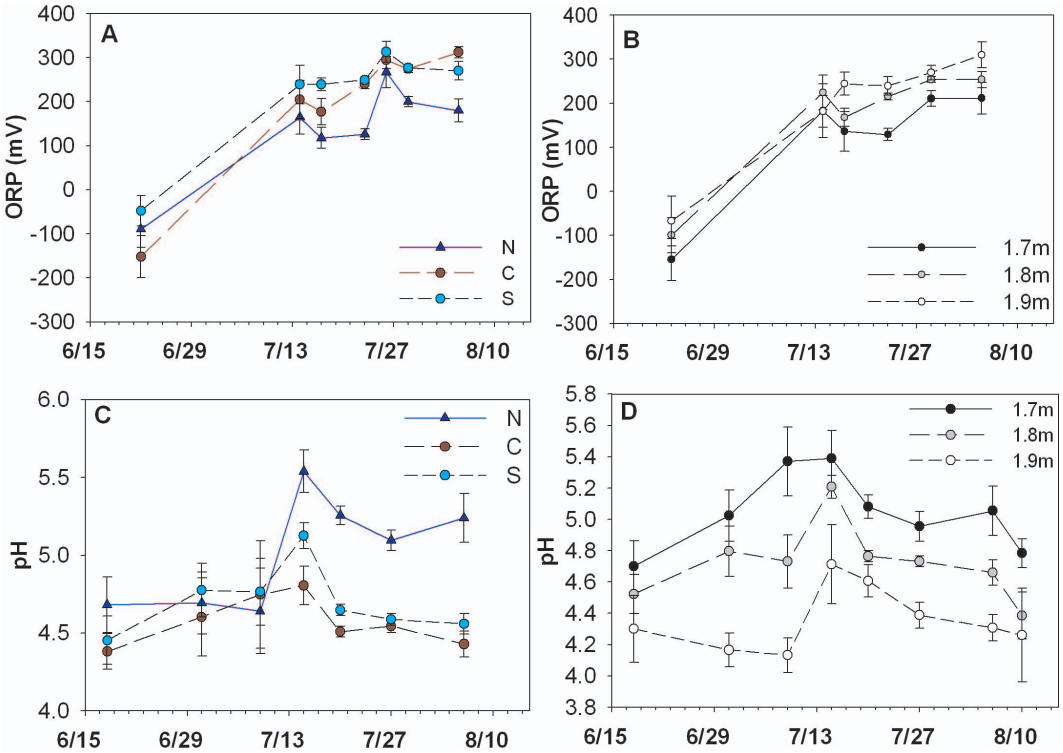

Fig. 3. Seasonal trends in 2009 for **(A)** ORP by transect, **(B)** ORP by elevation class, **(C)** pH by transect and **(D)** pH by elevation class. All electrochemical and temperature readings were taken at 10 cm depth. ORP values are relative to a Ag/AgCl reference electrode.

BGD
8, 6345–6382, 2011

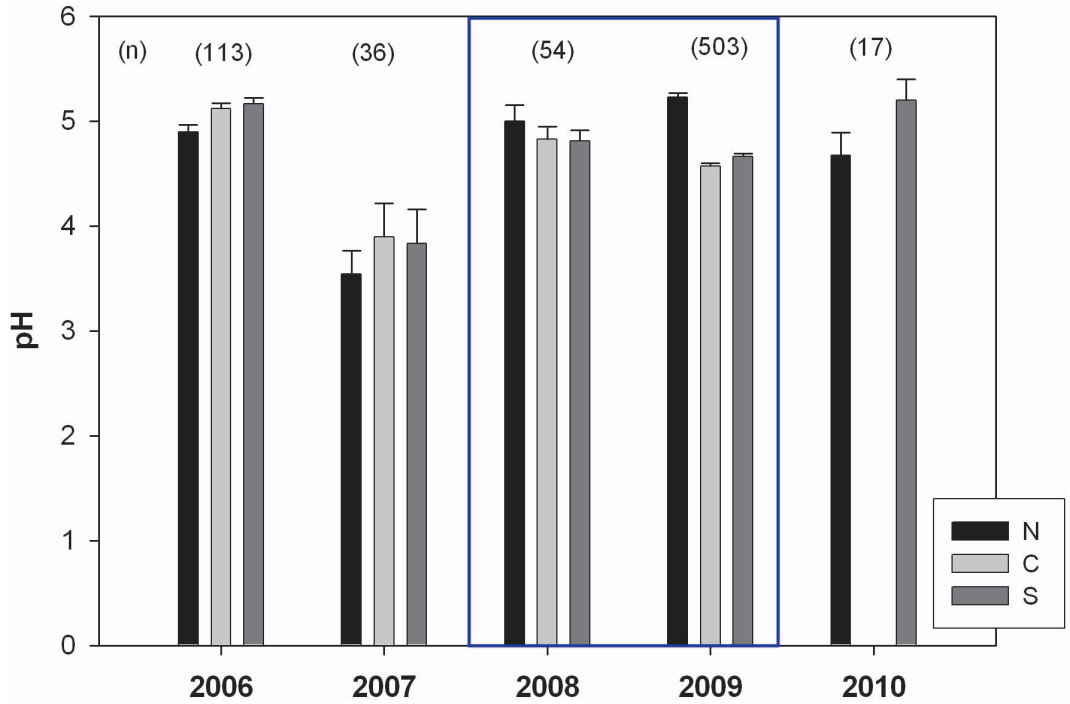

Fig. 4. Mean values (and standard errors) of pH before, during (blue box) and after flooding treatment along the three transects. Data shown are for mid July dates only (12 July–23 July).

BGD
8, 6345–6382, 2011

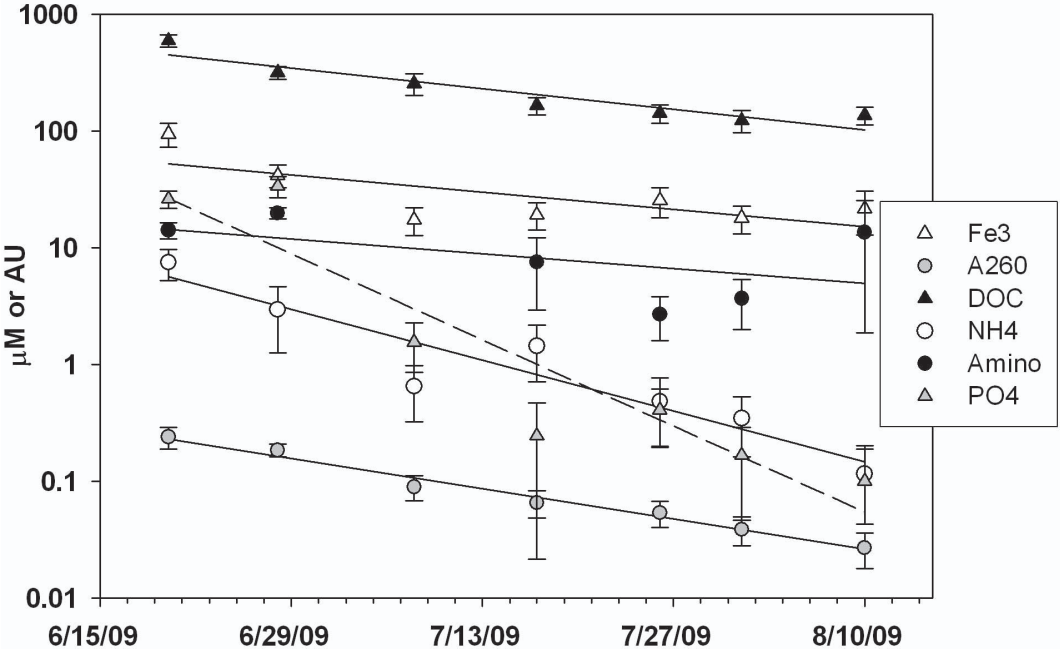

Fig. 5. Seasonal patterns of dissolved ion concentration (µm) and degree of UV absorbance (absorbance units, AU) in soil pore water collected from 0–5 cm depth in 2009. The y-axis is shown on a logarithmic scale.

BGD
8, 6345–6382, 2011

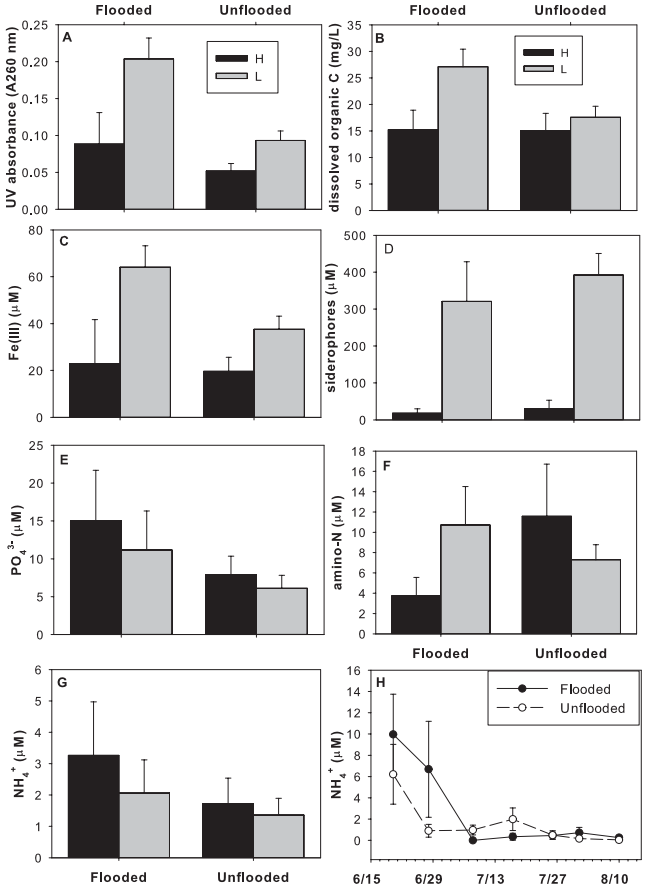

Fig. 6. Soil pore water chemistry extracted from upper 5 cm of soil in summer, 2009. **(A)–(G)** Grand means of all samples dates in summer 2009 in topographically high and low areas of flooded and unflooded treatments. Siderophore concentrations are presented as μm deferoxamine equivalents. **(H)** Seasonal trends for NH_4^+ in flooded and unflooded treatments.

BGD
8, 6345–6382, 2011

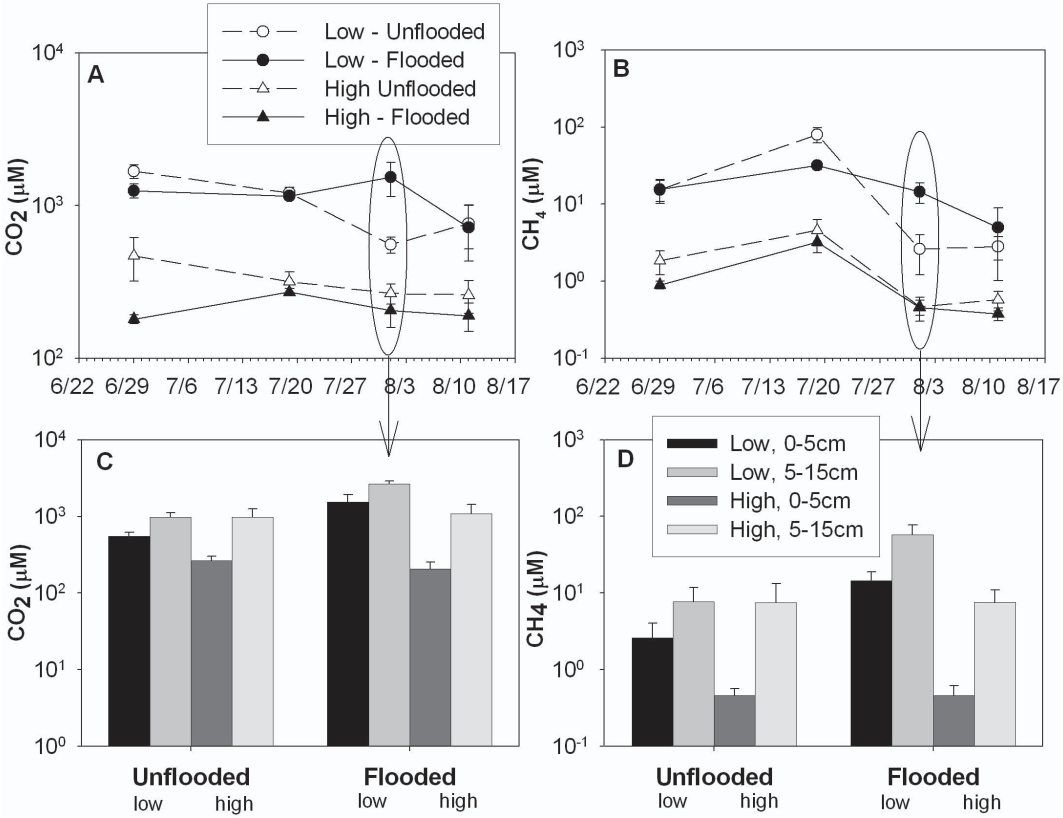

Fig. 7. Dissolved gases in soil pore water from high and low areas within flooded and unflooded treatments: **(A)** CO_2 and **(B)** CH_4 at a depth of 0–5 cm over four dates in 2009; **(C)** CO_2 and **(D)** CH_4 at 0–5 cm and 5–15 cm depth on 1 August 2009. The y-axes are scaled logarithmically.

BGD
8, 6345–6382, 2011

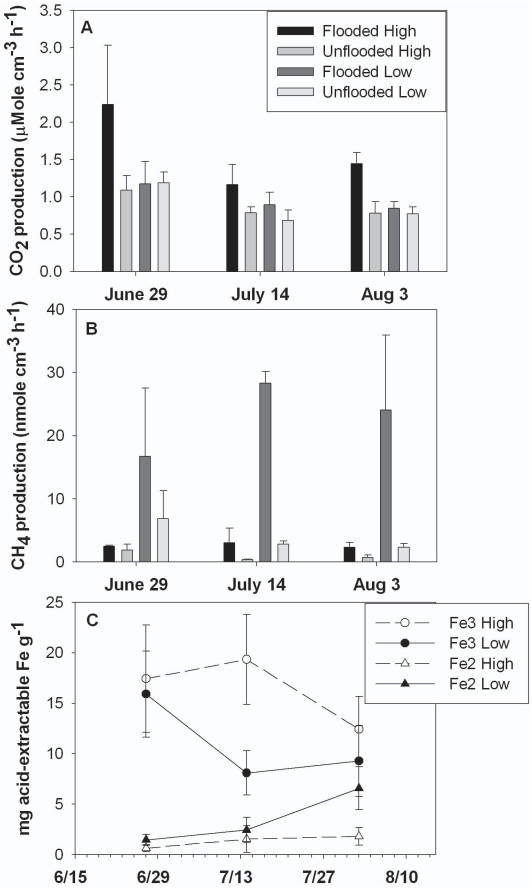

Fig. 8. Indicators of anaerobic processes in soils collected in 2009. Production rates of **(A)** CO_2 and **(B)** CH_4 in anaerobic laboratory incubations of soil from flooded and non-flooded treatments. **(C)** Seasonal changes in acid-extractable Fe(III) and Fe(II) from high and low areas of the landscape.

BGD
8, 6345–6382, 2011

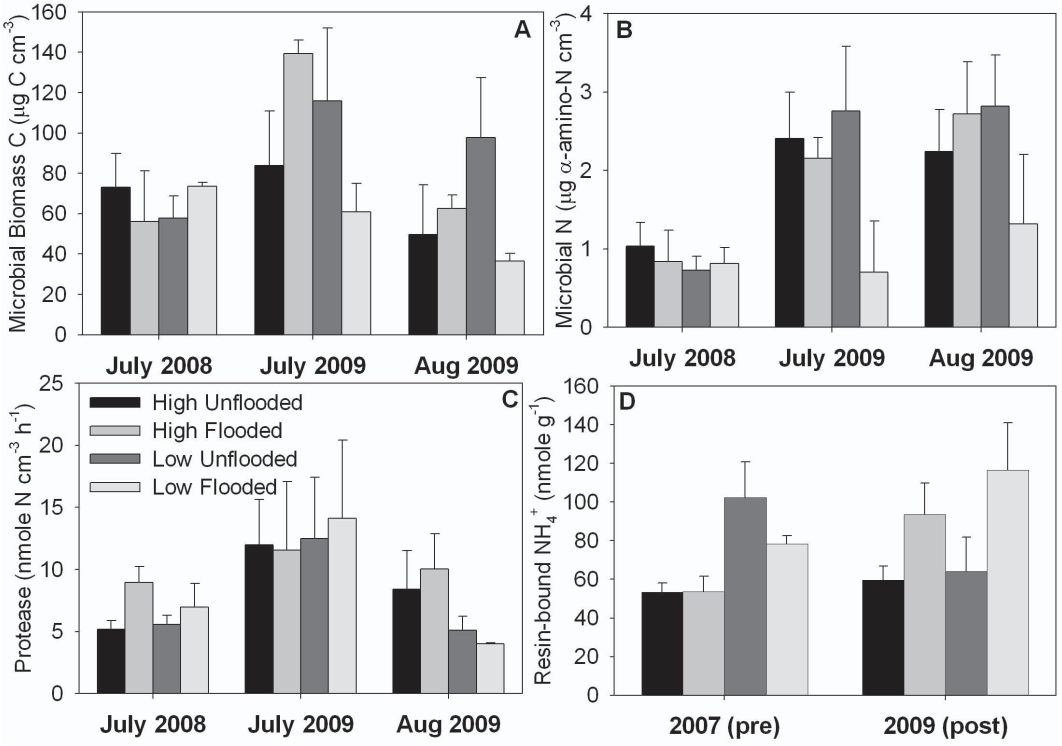

Fig. 9. Measures of microbial biomass and N cycling in soils collected from high and low areas of flooded and non-flooded areas: **(A)** microbial biomass C and **(B)** ninhydrin-active N measured by the fumigation-extraction method, **(C)** potential proteolysis rates, and **(D)** NH_4^+ bound to buried resin bags over the 2007 (pre-flooding) and 2009 (post-flooding) seasons.

BGD
8, 6345–6382, 2011

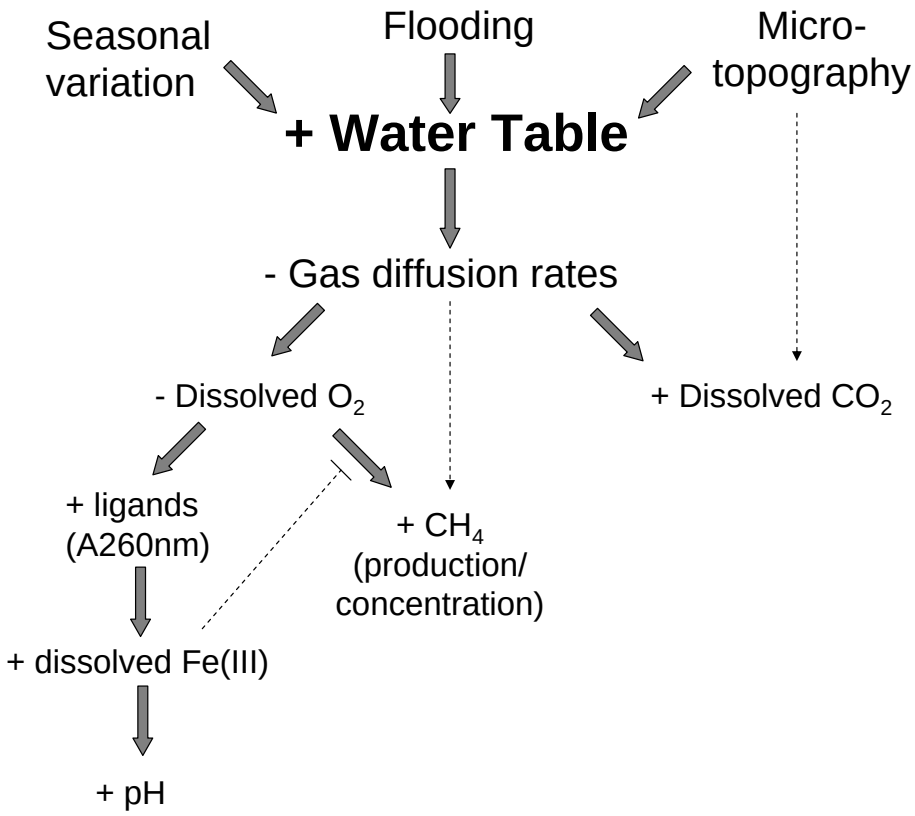

Fig. 10. Synthesis of major results from this paper, illustrating the most likely mechanisms by which water table affected the measured variables. The dotted flat arrow from Fe(III) to CH_4 indicates a possible negative effect.

BGD
8, 6345–6382, 2011